

# Reliable 3D astrocyte spheroid model systems

## Introduction

A recently published article, which attracted significant attention in the scientific community, revealed that SARS CoV-2 infects brain astrocytes and can trigger neuropathological changes. [1] Astrocytes are the most numerous cell population in the central nervous system and located in direct neighborhood of neuronal synapsis; they are amenable for neurotransmitter recycling but also control synapse formation, function, and removal. Due to their indispensable role in neuronal information processing and physiological brain function, both their relevance in neurotoxic effects (e.g. SARS CoV-2) and in neurodegenerative disorders such as Amyotrophic Lateral Sclerosis needs to be assessed. [2, 3] However, examining the function of astrocytes in brain diseases is remarkably challenging in human beings. [4] Due to the donor limitations of human primary brain tissue and complex *in vitro* culture of primary astrocytes and organoids, most fundamental insights were discovered in animal models while taking interspecies differences into account. The complexity of human astrocytes in their development, morphology, and functionality is significantly greater than in other species-derived counterparts. Furthermore, looking at molecular construction, human astrocytes' transcriptome encodes for hundreds of more genes than in other species. [2]

In order to achieve a greater understanding of brain infections due to COVID-19, new *in vitro* models have been implemented, however with inconsistent results. SARS-CoV-2 infections of 2D cell-based models showed a low infection rate of neurons and astrocytes in comparison to abundant infection of genetically engineered human induced pluripotent (hiPSC)-derived astrocytes and neurons. Furthermore, when implementing more complex structures such as 3D brain organoids, the infection rate was dependent on cellular components. [5] Viral RNA level was higher in infected brain organoids cocultured with astrocytes compared to cultures without astrocytes. [6] These findings underline the high demand for reliable brain model systems, including astrocytes, which can help to understand current disease pathways.



Three-dimensional *in vitro* cell culture systems based on human immortalized cell lines provide the potential to overcome the limitations of human primary cells, long and complicated culturing procedures of primary cells and organoids, and to fill in any information gaps between animal experiments and human beings.

Culturing human astrocytes in 3D cell spheroids imitates the dense cell network *in vivo* by allowing cell-cell contact in all dimensions. Generating consistent cell spheroids requires a cell- and protein-repellent environment forcing the cells to aggregate and form a 3D structure. This environment is provided by specially treated cell culture equipment, which can differ in performance in terms of spheroid formation time, viability, and functionality and thereby impacting the assays' read-out.

In the current study, we established a 3D spheroid model with human immortalized astrocytes on BIOFLOAT™ 96-well plates which allows the investigation of human astrocytes in health and disease. For this purpose, the usage of defined, fully inert, animal-free low-attachment plates for spheroid formation were investigated in terms of formation time and spheroid viability to find the most reliable basic conditions for establishment of *in vitro* models.

## Materials and Methods

### *Standard Cell Culture*

Human immortalized astrocytes, CI-huAstro (clone “SFFV2”; InSCREENeX GmbH; INS-CI-1023) were cultured on Poly-L-Lysine coating solution (InSCREENeX GmbH; INS-SU-1019) coated cell culture flasks in huAstro medium (InSCREENeX GmbH; INS-ME-1030) at 37°C and 5% CO<sub>2</sub>. For cell maintenance and cell expansion, medium was exchanged every 2-3 days and cells were splitted at 80-90% confluency.

### *Spheroid formation*

For generation of cell spheroids, 10 000 cells/well were seeded into BIOFLOAT™ 96-well plates (faCellitate, Germany) and two other commercially available low-attachment plates (benchmark 1 U-bottom, benchmark 2 F-bottom). Spheroids were cultured up to 9 days at 37°C and 5% CO<sub>2</sub>.



### *Morphology analysis*

The morphology of the cells was analyzed on day 1, 3, 7, and 9 post-seeding. For this purpose, spheroids were imaged using Incucyte<sup>R</sup> S3 (Sartorius) and analyzed via ImageJ (Wayne Rasband, public domain) macro with image processing followed by automatic segmentation, diameter, and circularity calculation. For analysis, images of three biological replicates (at least one passage and/or cryopreservation between experiments) including 48 technical replicates (single spheroids or wells of 96-well plate) were used.

### *Time lapse analysis*

For time lapse analysis, 10 000 astrocytes/well were seeded into BIOFLOAT<sup>TM</sup> 96-well plates and two other commercially available low-attachment plates and imaged every hour using Incucyte<sup>R</sup> S3 imaging system. Spheroid formation of six spheroids per plate were analyzed using ImageJ. For this purpose, the percentage of cell aggregate-free areas within the formed spheroid were measured. A low percentage of cell free areas indicated a dense structure within the spheroid.

### *Viability analysis*

To test the viability of spheroids after 3 and 9 days of culture, ATP level of cells were measured using Promega CellTiter-Glo 3D (Promega) according to the manufacturer's instructions. Samples of three biological replicates with 18 to 24 technical replicates were used.

### *Fluorescent viability analysis*

For visualization of cell viability, live cells within the spheroid were stained with Calcein AM (ThermoFisher Scientific) and dead cells were stained with Propidium Iodide (PI) nucleic acid (ThermoFisher Scientific) according to the manufacturer's instructions. Calcein AM is converted into green fluorescent calcein by intracellular hydrolysis indicating viability of the cells. Dead cells are permeable for PI, which binds to DNA by intercalating between the bases. Samples of three biological replicates including 12 technical replicates were stained.

### *Immunofluorescent staining for astrocyte marker*



The surface marker S100 Calcium Binding Protein B (S100B) and Glial Fibrillary Acidic Protein (GFAP) on human astrocytes were stained using anti-S100B (Synaptic Systems; Polyclonal rabbit anti-S100B) and anti-GFAP (Synaptic Systems; Monoclonal mouse anti-GFAP) after 3 days of culture. S100B is a frequently used marker protein for mature astrocytes, whereas GFAP is also expressed in germinal zone cells that maintained their immature developmental stage. Prior to antibody staining, cells were fixed with 4% (w/v) paraformaldehyde in PBS (pH 7.4) for 15 - 20 min at room temperature. Afterwards, fixed spheroids were washed three times with PBS for 10 min and incubated for 30 min in blocking buffer (10% (v/v) serum/ 0.1% (v/v) Triton X100 in PBS). Primary anti-S100B and anti-GFAP antibodies were diluted in blocking buffer and samples were incubated for 2h at room temperature. Samples were then washed three times with PBS for 10 min and incubated in secondary antibody solution (Goat IgG anti-Mouse IgG+IgM (H+L)-Cy3, Dianova and Goat F(ab')<sub>2</sub> anti-Rabbit IgG (H+L)-Cy3, Dianova in blocking buffer) for 1h at room temperature. After three washing steps, spheroids were covered with mounting medium including DAPI and observed under microscope. Astrospheroids of four biological replicates were stained.

## Results

### *Rapid and compact astrocyte spheroid formation on BIOFLOAT™ plates*

Spheroid generation time can be an important factor for time-dependent experiments as well as for drug testing studies in which reducing days of analysis can shorten the preclinical phase. Therefore, we analyzed the spheroid formation within 24 h using time lapse images. In BIOFLOAT™ plates, astrocytes started to aggregate within the first hour of culture and showed 24.6 % cell-free area within cell aggregates (cell-free area, Figure 2A). Within 9 h of culture, astrocytes in BIOFLOAT™ plates and Benchmark 1 rapidly formed a network of cells with smaller cell free area (8.8% BIOFLOAT™ and 9.8% benchmark 1), faster than cells cultured in Benchmark 2. Astrocyte spheroids in Benchmark 2 revealed 11% cell-free area after 9 h, indicating a loose structure of aggregates, which densified to a compact structure with 1.23% of cell-free area after 22 h of culture. The lowest percentage of cell free area (0.54%) was achieved for astrocytes cultivated in BIOFLOAT™ after one day, which resulted in a dense spheroid. BIOFLOAT™ triggered the fastest formation of astrocytes into round spheroids within 22 h. The morphology of these generated astrospheroids was further analyzed for



consistency since the spheroids' shape may be a source of variability in read-out of experiments. [7] Analysis of images of cell spheroids in BIOFLOAT™, Benchmark 1, and Benchmark 2 revealed that spheroids lose their shape starting from day 7 (Figure 1).

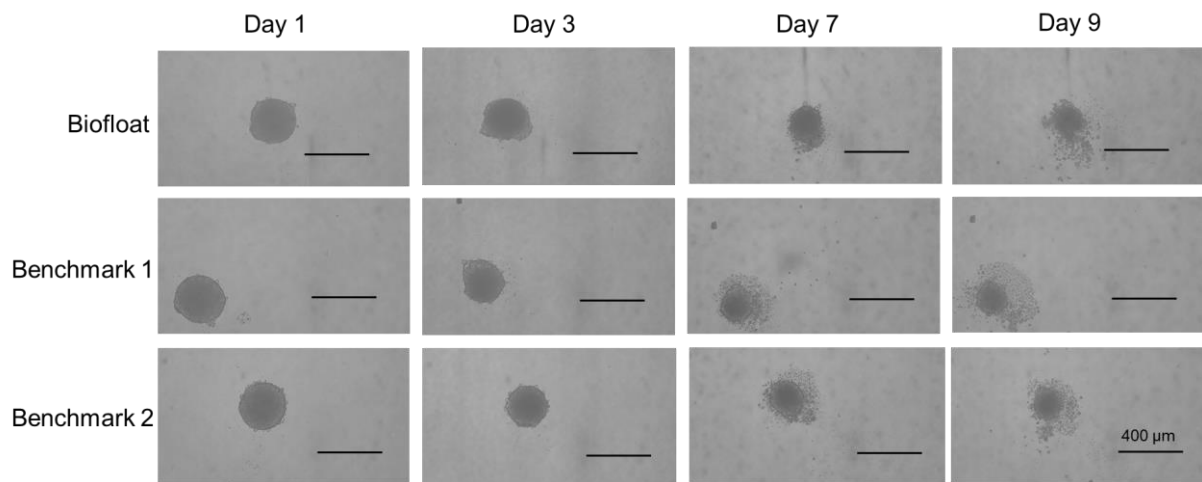


Figure 1 Microscopic images of astrocyte spheroids products. Spheroids were cultured in BIOFLOAT™ 96-well plates (first row) and two benchmark products (second and third row) up to 9 days and imaged on day 1,3,7, and 9. Scale: 400  $\mu\text{m}$ .

These morphological changes were quantified by measurements of diameter, circularity, and solidity on days 1, 3, 7, and 9 (Figure 2). For all conditions, the diameter of astrospheroids increased with time as would be expected. On day 1, cells in BIOFLOAT™, Benchmark 1, and Benchmark 2 formed spheroids with a size of  $300.4 \pm 8.7 \mu\text{m}$ ,  $292.0 \pm 20.1 \mu\text{m}$ , and  $306.6 \pm 7.6 \mu\text{m}$ , respectively. Spheroid diameter increased with time in all conditions and astrospheroids cultured in BIOFLOAT™ reached an intermediate diameter of  $345.1 \pm 8.4 \mu\text{m}$  after 9 days of culture between Benchmark 2 ( $376.3 \pm 39.1 \mu\text{m}$ ) and Benchmark 1 ( $306 \pm 11.8 \mu\text{m}$ ) The low circularity value of spheroids in Benchmark 1 ( $0.82 \pm 0.05$ ) after day 1 were consistent with the results of time lapse analysis, where cells aggregated into spheroids with irregular shape. In contrast, spheroids with a high level of circularity, indicating a perfect round shape, were generated in BIOFLOAT™ and Benchmark 2. Furthermore, the circularity of spheroids decreased after day 9 to a value of  $0.8 \pm 0.2$  for BIOFLOAT™,  $0.8 \pm 0.04$  for Benchmark 1, and  $0.8 \pm 0.02$  for Benchmark 2, reflecting the cells' tendency to disassemble into a loose structure of spheroids. For description of the outer rim of astrospheroids, the solidity was measured. Astrospheroids cultured in BIOFLOAT™ and Benchmark 2 showed a more regular defined cell border quantified by a solidity value of  $0.98 \pm 0.0009$  and  $0.98 \pm 0.003$ , respectively, compared to Benchmark 1 ( $0.96 \pm 0.019$ ). In all conditions, solidity decreased over time in accordance to the observations obtained from circularity and diameter



results. Zaroni et al. previously published data indicating that selecting homogeneously-shaped spheroids for reducing data variability is important in cytotoxicity analysis. [7] BIOFLOAT™ and Benchmark 2 allowed the fastest generation of round, uniform astrospheres within 24 h and revealed a uniform spheroid shape, making them ideal for cytotoxicity analysis.

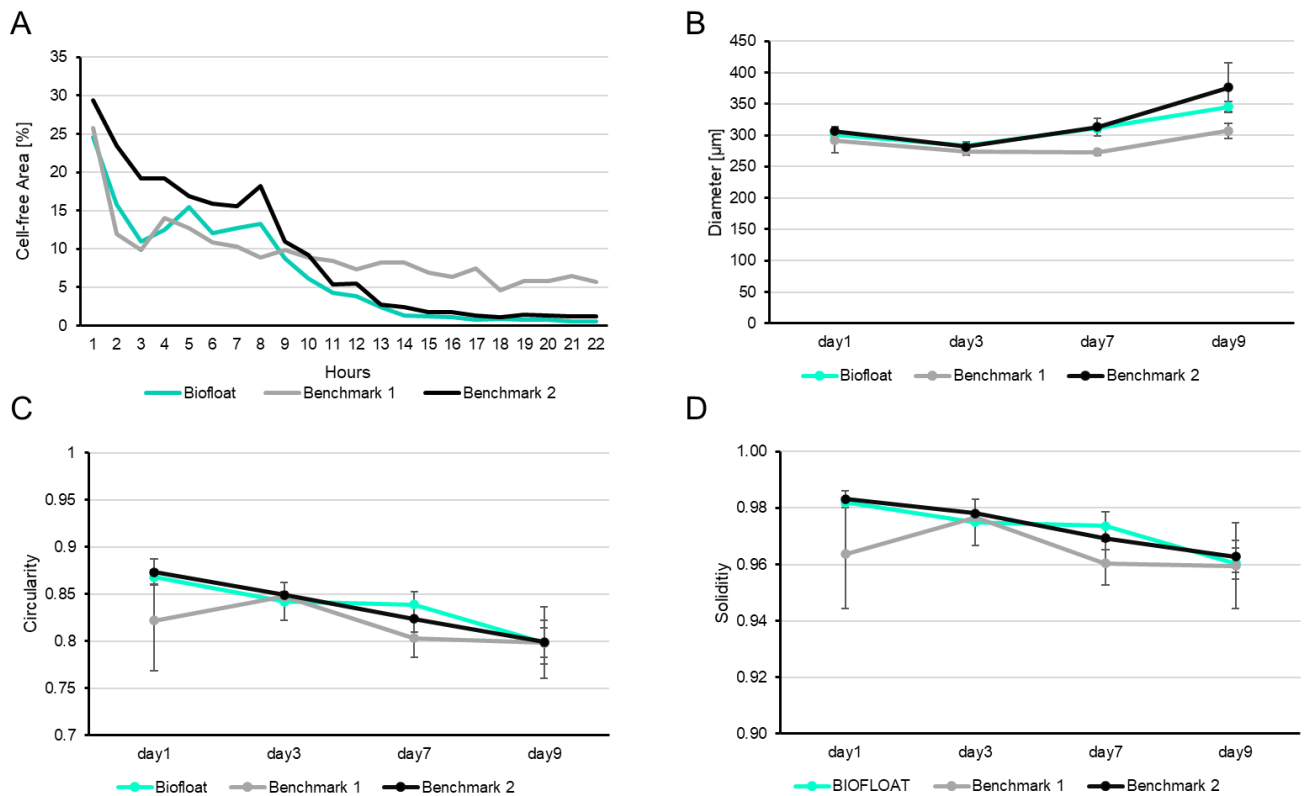


Figure 2 Analysis of formed spheroids in BIOFLOAT™, Benchmark 1, and Benchmark 2. Spheroid formation was pursued for 22 h using time lapse movies and analyzed by determining the cavities between the cell during spheroid formation (A). Diameters (B), Circularity (C), and Solidity (D) of imaged spheroids in BIOFLOAT™, Benchmark 1 and Benchmark 2 were measured at 1, 3, 7 and 9 days after seeding.

### Highly viable cell spheroids on BIOFLOAT™ plates

The use of viable 3D spheroids in *in vitro* testing systems is one important factor when investigating the effect of external factors (e.g., drugs, toxins) on cell apoptosis. More importantly, the viability of astrocytes within one spheroid was analyzed to determine the optimal cell culture condition of the 3D model. The cell viability was quantified by measuring the intracellular ATP level. For this purpose, astrocytes were lysed after 3 and 6 days of culture and the supernatant was analyzed as summarized in Figure 3A. Surprisingly, the luminescence values, indicating the amount of ATP in cultured cells, were significantly higher in BIOFLOAT™



plates on day 3 (2277187 +/-195286.6) and day 6 (2120218 +/- 164880.9) than for the benchmark products (Figure 3A). These results were also confirmed by microscopic fluorescence images, which showed more viable cells (green) on day 3 in BIOFLOAT™ plates than in spheroids cultured in Benchmark products (Figure 3B). In contrast, the viability of astrospheroids in Benchmark 1 decreased to the lowest value at day 6 (1868463 +/- 1161997). Endpoint analysis (day 9) of spheroids using fluorescence marker for viable and dead cells revealed a viable core of spheroids cultured in BIOFLOAT™ plates with some dead astrocytes loosely populated around the viable spheroid core. The same phenomenon was visible for astrocytes cultured for 9 days in both Benchmark products. In combination with the morphological analysis, these results imply that dead cells leave the dense spheroid structure after 9 days of culture, leading to a disassembled, loose structure. In any case, BIOFLOAT™ plates support the formation and maintenance of highly viable spheroids, which is an optimal prerequisite for qualified analysis of cellular response regarding cell apoptosis.

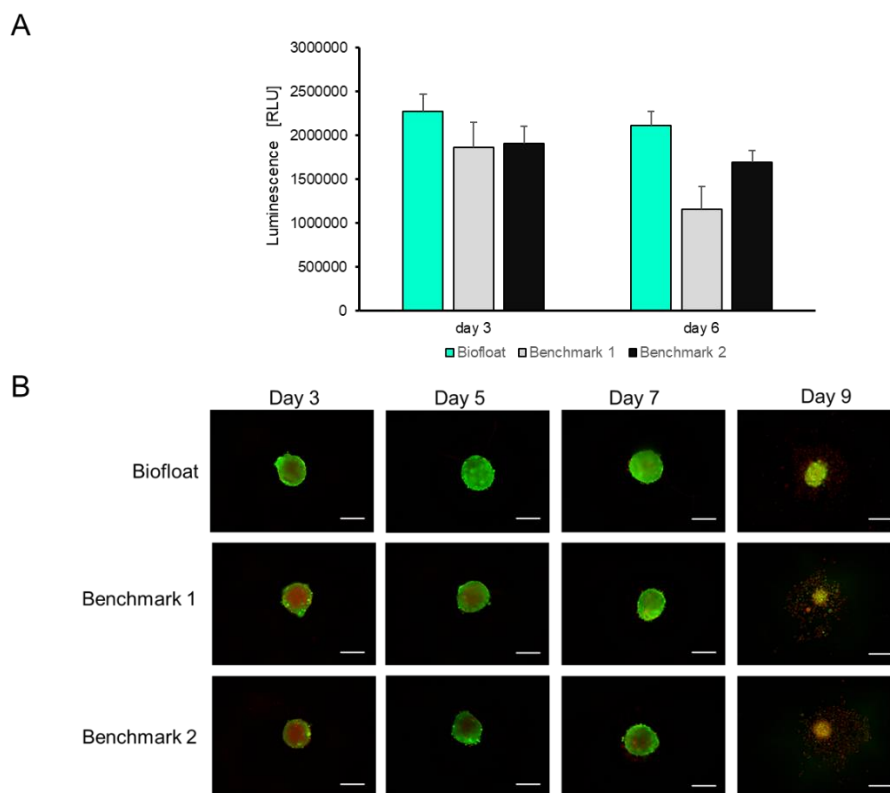


Figure 3 Viability analysis of astrocyte spheroids. ATP level of spheroid cultures in BIOFLOAT™, Benchmark 1 and Benchmark 2 were measured by luminescence signal detection using Cell titer Glo (A). For visualization of cell viability, spheroids were stained with calcein (green) showing viable cells and dead cells were stained with PI (red) (B). Scale bar:200 µm.

*Astrospheroids express typical marker of astrocytes*



Human astrocyte phenotype was evaluated by staining of typical markers S100B and GFAP (Figure 4). Both markers are constantly expressed by cells within the spheroids in BIOFLOAT™, Benchmark 1, and Benchmark 2. S100B, produced mainly by astrocytes, plays a crucial role in the astrocyte activation process, migration, and cell shape. [8] Further upregulation of GFAP is linked to neuronal damages and is an indicator for brain injury. [9, 10] Therefore, both markers are suitable for identification of astrocytes and for cell analysis regarding cell behavior. In all conditions, astrospheroids express these hallmarks of astrocytes, indicating a stable cell line for astrospheroid formation.

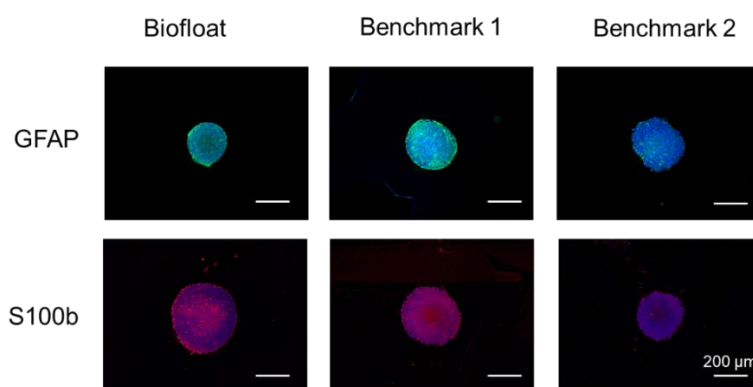


Figure 4 Immunofluorescence staining of astrospheroids. Cells in BIOFLOAT, Benchmark 1, and Benchmark 2 were stained against the surface marker GFAP (1<sup>st</sup> row) and S100B (red, 2<sup>nd</sup> row).

## Conclusion

Establishment of 3D astrocyte cultures can address a wide range of applications and answer fundamental questions in the field of neurodegenerative diseases or as model systems for toxicological screening purposes. Implementation of immortalized astrocytes in such 3D cultures can provide the ability to overcome the gap between current model systems with insufficient reproducibility or transferability to humans and the lack of human donor cells. For this purpose, we established 3D astrospheroid model systems in different cell culture plates and evaluated their morphology and vitality. Astrocyte spheroids were formed in all products, indicating the suitability of this cell line for spheroid formation. In BIOFLOAT™ plates, cell spheroids were formed remarkably fast and revealed spheroids with a larger diameter, circularity, and solidity than compared spheroids produced in Benchmark 1. Therefore, BIOFLOAT™ plates are well suited for analysis in the first days of culture when a high degree of consistency is needed to accelerate experiments. Furthermore, BIOFLOAT™ plates



outperformed both Benchmark products in the viability of generated spheroids, which qualifies them for applications in which the performance is evaluated by reduced viability such as drug testing systems. In conclusion, easy-to-use BIOFLOAT™ 96-well plates allow fast growth of perfect, round astrocyte spheroids in a chemically defined, fully inert and animal-free environment. Successful implementation of 3D astrospheroid as *in vitro* models for neurodegenerative diseases or brain infections or neurodegenerative diseases caused by COVID-19 provides the potential to overcome the inconsistent results of current *in vitro* models.

For additional information, please visit [www.faCellitate.com](http://www.faCellitate.com) or contact us at

Chemovator GmbH

Industriestraße 35

68169 Mannheim, Germany

T +49 621 60 29872

info@facellitate.com

## References

1. Crunfli, F., et al., *SARS-CoV-2 infects brain astrocytes of COVID-19 patients and impairs neuronal viability*. medRxiv, 2020: p. 2020.10.09.20207464.
2. Tyzack, G., A. Lakatos, and R. Patani, *Human Stem Cell-Derived Astrocytes: Specification and Relevance for Neurological Disorders*. Current Stem Cell Reports, 2016. **2**(3): p. 236-247.
3. Herculano-Houzel, S., *The glia/neuron ratio: how it varies uniformly across brain structures and species and what that means for brain physiology and evolution*. Glia, 2014. **62**(9): p. 1377-91.
4. Phatnani, H. and T. Maniatis, *Astrocytes in neurodegenerative disease*. Cold Spring Harbor perspectives in biology, 2015. **7**(6): p. a020628.
5. Trevisan, M., et al., *SARS-CoV-2 Infection and Disease Modelling Using Stem Cell Technology and Organoids*. International Journal of Molecular Sciences, 2021. **22**(5): p. 2356.
6. Wang, C., et al., *ApoE-Isoform-Dependent SARS-CoV-2 Neurotropism and Cellular Response*. Cell Stem Cell, 2021. **28**(2): p. 331-342.e5.
7. Zanoni, M., et al., *3D tumor spheroid models for in vitro therapeutic screening: a systematic approach to enhance the biological relevance of data obtained*. Scientific Reports, 2016. **6**(1): p. 19103.
8. Brozzi, F., et al., *S100B Protein Regulates Astrocyte Shape and Migration via Interaction with Src Kinase: IMPLICATIONS FOR ASTROCYTE DEVELOPMENT, ACTIVATION, AND TUMOR GROWTH*. The Journal of biological chemistry, 2009. **284**(13): p. 8797-8811.
9. Dong, J., et al., *Quantification of Astrocytes and GFAP-Immunoreactivity in Normal and Glaucomatous Human Retinas*. Investigative Ophthalmology & Visual Science, 2002. **43**(13): p. 4072-4072.
10. Rosa, J.M., et al., *Microglia-to-astrocyte communication modulates synaptic and cerebrovascular functions following traumatic brain injury*. bioRxiv, 2020: p. 2020.03.01.972158.

